Biophysical Journal, Volume 97

Supporting Material

Membrane Curvature Induced by Aggregates of LH2s and Monomeric LH1s

Danielle E. Chandler, James Gumbart, John D. Stack, Christophe Chipot, and Klaus Schulten

Supporting Material

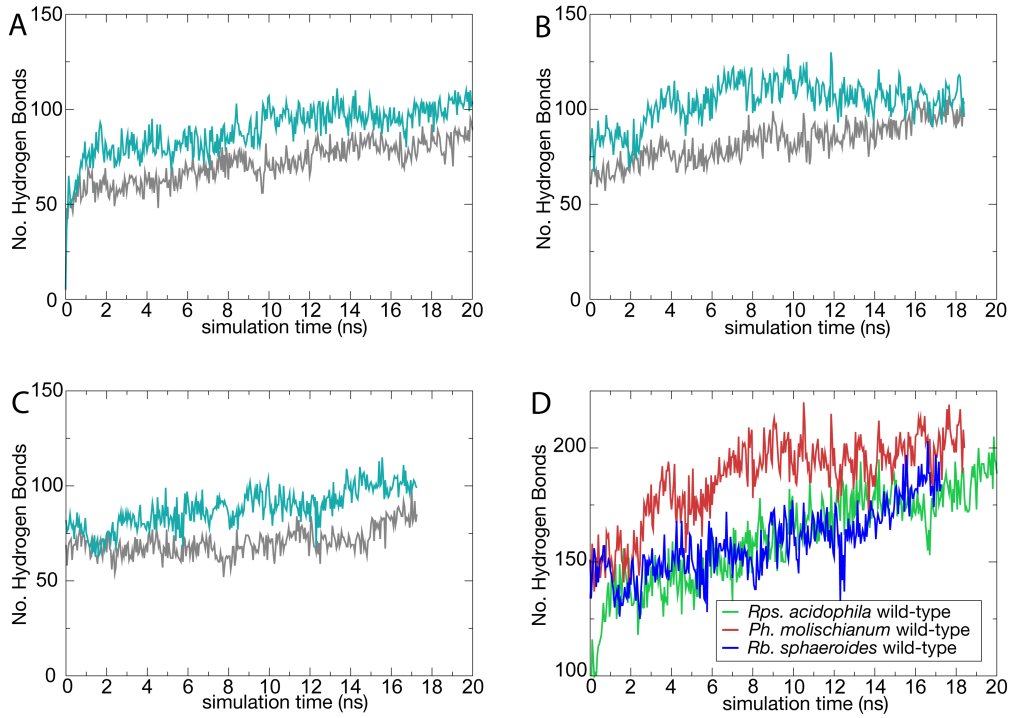

Figure S1: Hydrogen bonds formed between protein and lipids over time. In A, B, and C, grey represents bonds formed with POPE and cyan represents bonds formed with POPG for LH2 from A) *Rps. acidophila*, B) *Ph. molischianum*, and C) *Rb. sphaeroides*. D) Comparison by species of hydrogen bonds formed between protein and all lipids over time.

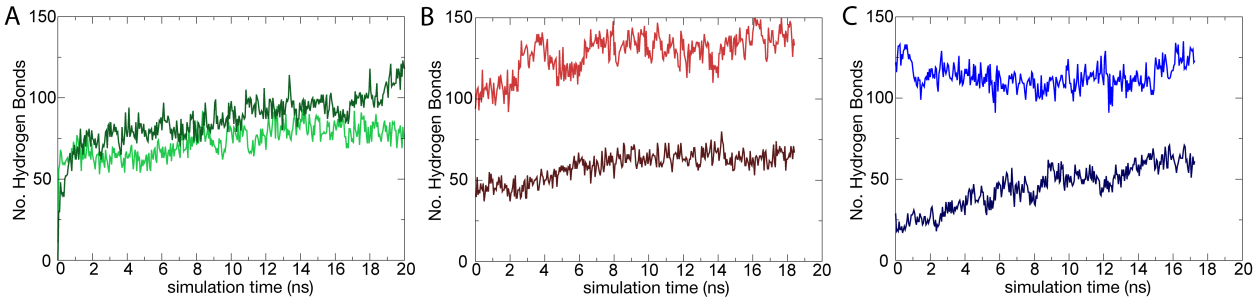

Figure S2: Hydrogen bonds formed with lipids for the cytoplasmic (light-colored line) and periplasmic (dark-colored line) halves of LH2 from A) *Rps. acidophila*, B) *Ph. molischianum*, and C) *Rb. sphaeroides*.

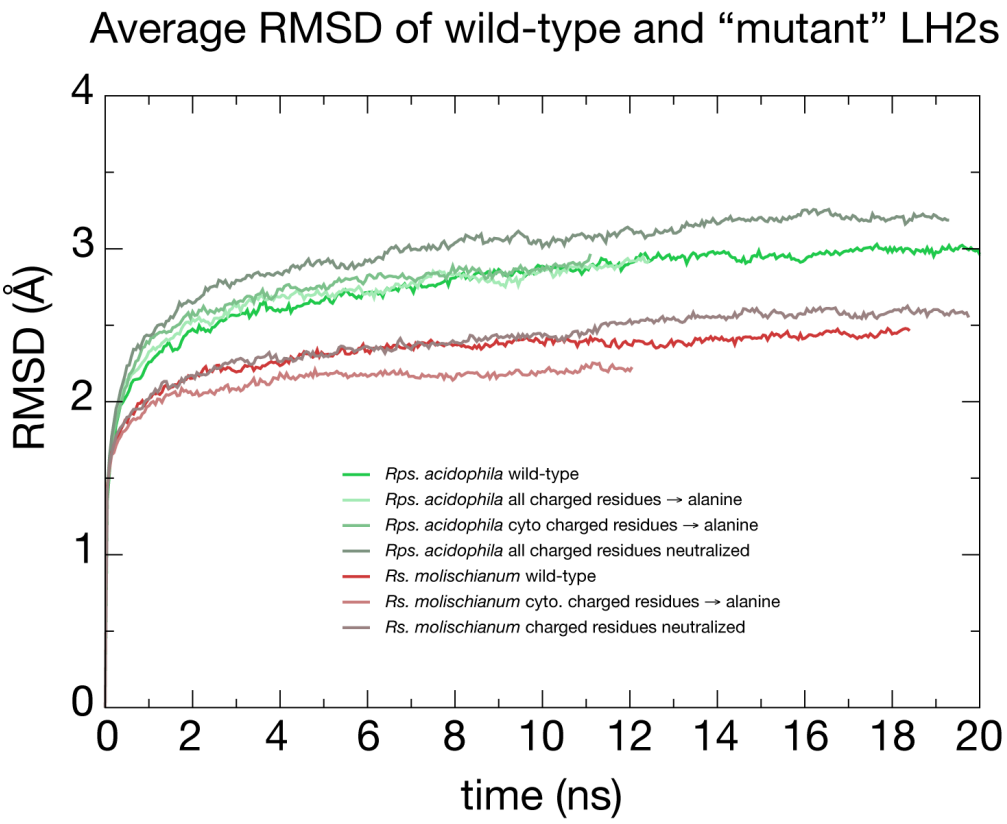

Figure S3: Average root mean-square deviation (RMSD) of the seven LH2s in the simulation system, plotted over the trajectory. The RMSDs of the “mutant” LH2s are similar to those of the unmodified LH2s, showing that the modification to the structure did not destabilize the proteins on the timescales reached in the simulations.

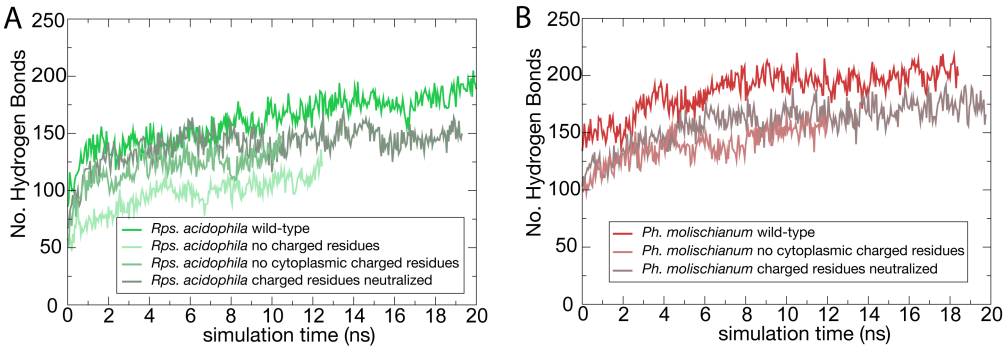

Figure S4: Comparison of hydrogen bonds formed between lipids and A) *Rps. acidophila* mutants and B) *Ph. molischianum* mutants.

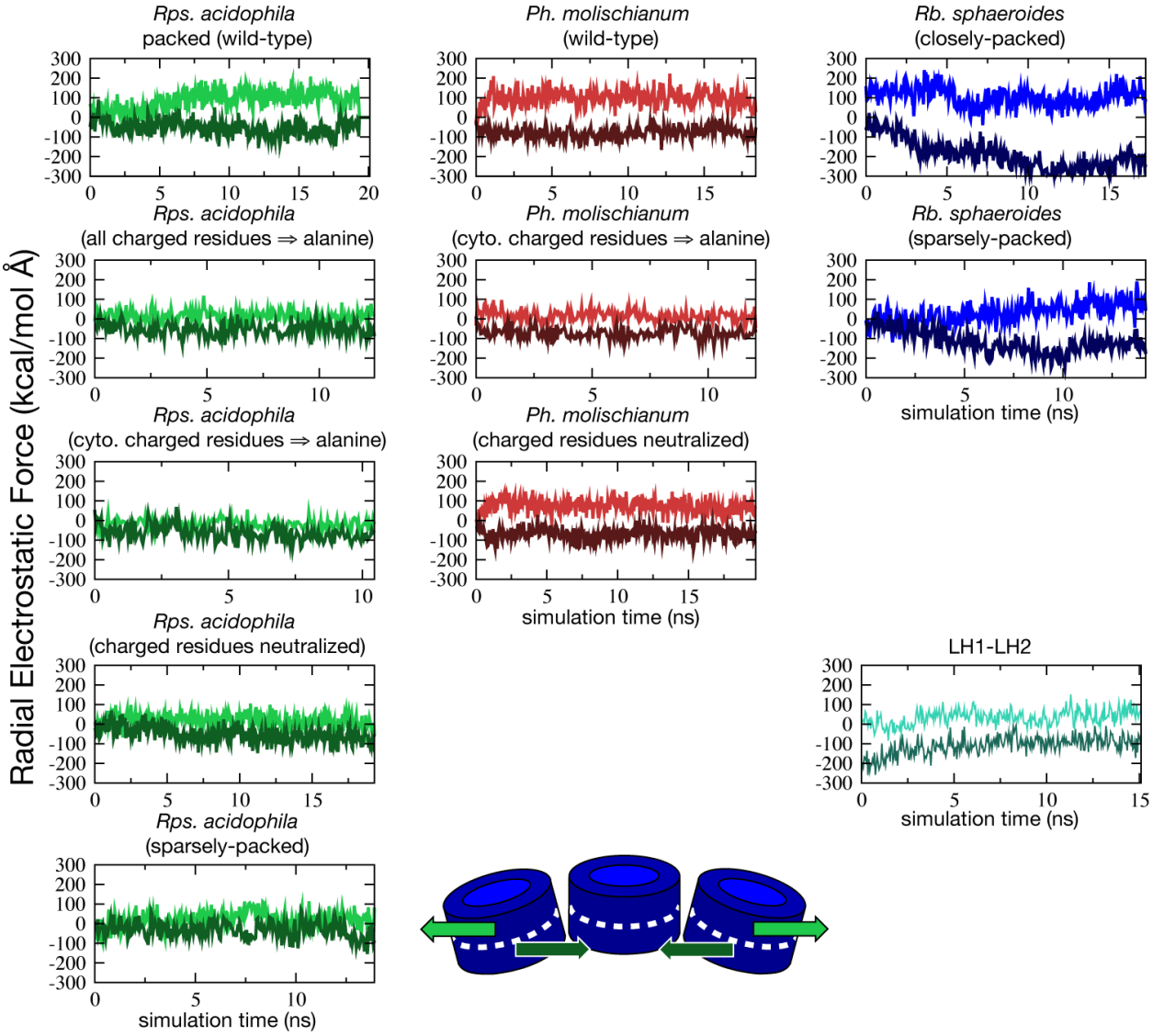

Figure S5: Average radial electrostatic force on the top (cytoplasmic) and bottom (periplasmic) sections of an outer ring LH2. The forces plotted are the electrostatic interaction forces (in kcal/mol·Å) between the other six LH2s plus surrounding water, lipids, and ions, and the top or bottom section of the LH2, projected onto the radial vector between the central LH2 and the outer ring LH2 on which the force is being calculated. A positive value then indicates a radially outward force while a negative value indicates a radially inward force. In all of the LH2-LH2 simulations, we observe that the force on the top of the LH2 (light-colored line) is outwards and the force on the bottom (dark-colored line) is inwards, i.e. they would produce the tilting behavior seen in the simulations. The simulations which show the greatest tilt angle also consistently display the largest forces. The inset cartoon illustrates this configuration of forces. The LH1-LH2 simulation gives the force on both halves of the LH2 as directed inwards, with the bottom force initially larger than the top force at the beginning of the simulation, but equal to the top force for the remainder of the time; such forces are consistent with the very small tilt angle that develops in the LH1-LH2 simulation.

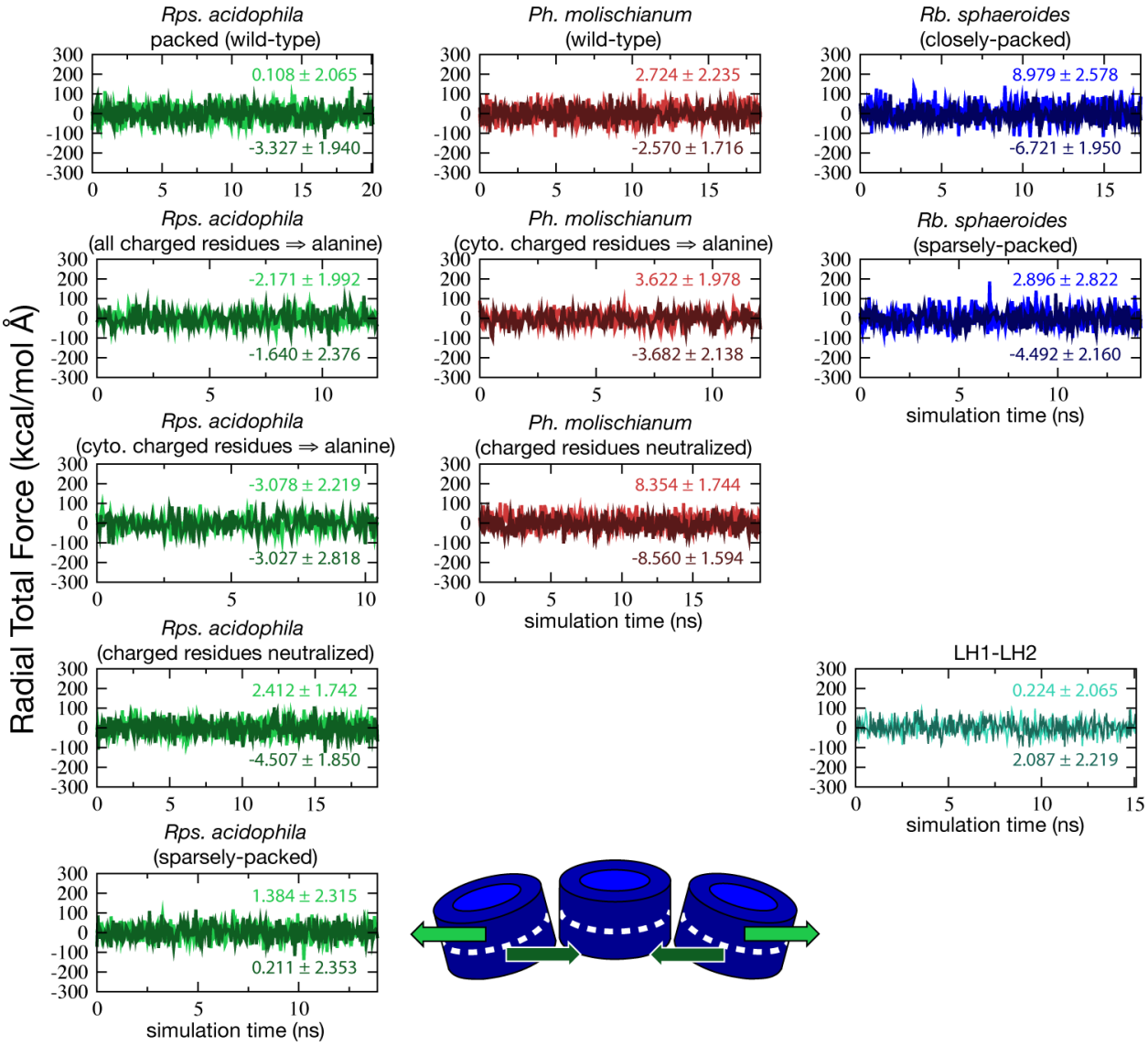

Figure S6: Total force in kcal/mol·Å (van der Waals plus electrostatics) experienced by an outer ring LH2, projected onto the radial vector connecting it to the central LH2. In each case, the van der Waals forces nearly cancel the electrostatics forces, but a small average force remains. The forces on the top and bottom halves of the LH2 are again such that would produce curvature, except in the *Rps. acidophila* "mutant" cases, where the curvature produced is nearly zero.

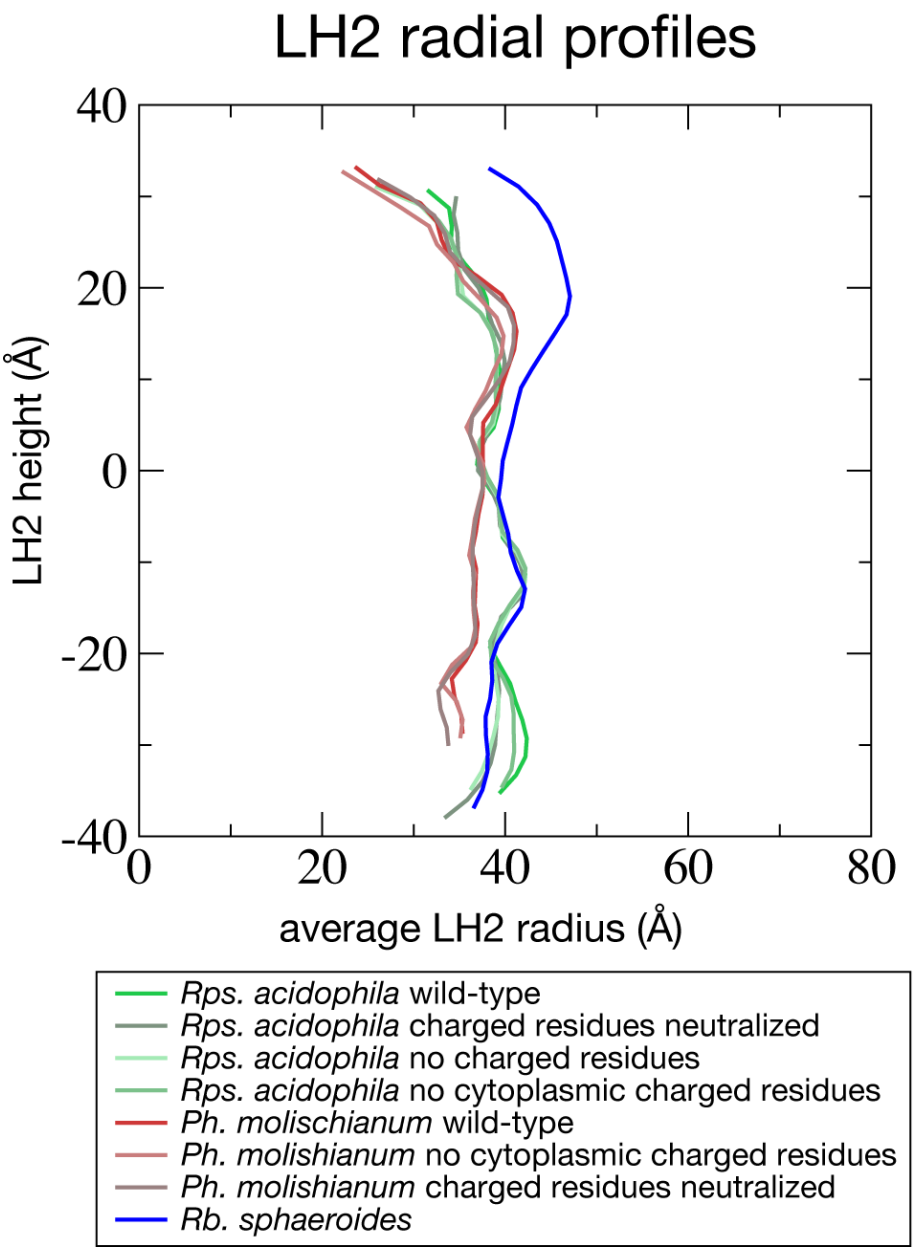

Figure S7: Radial profile of each LH2 protein simulated. Radii are averaged over the trajectory and over each of the seven LH2s in the simulation. The cytoplasmic protrusions of *Ph. molischianum* and *Rb. sphaeroides* are clearly seen, in contrast to the more cylindrical shape of *Rps. acidophila*. The shape of the "mutant" LH2 versions are slightly altered from the wild-types.

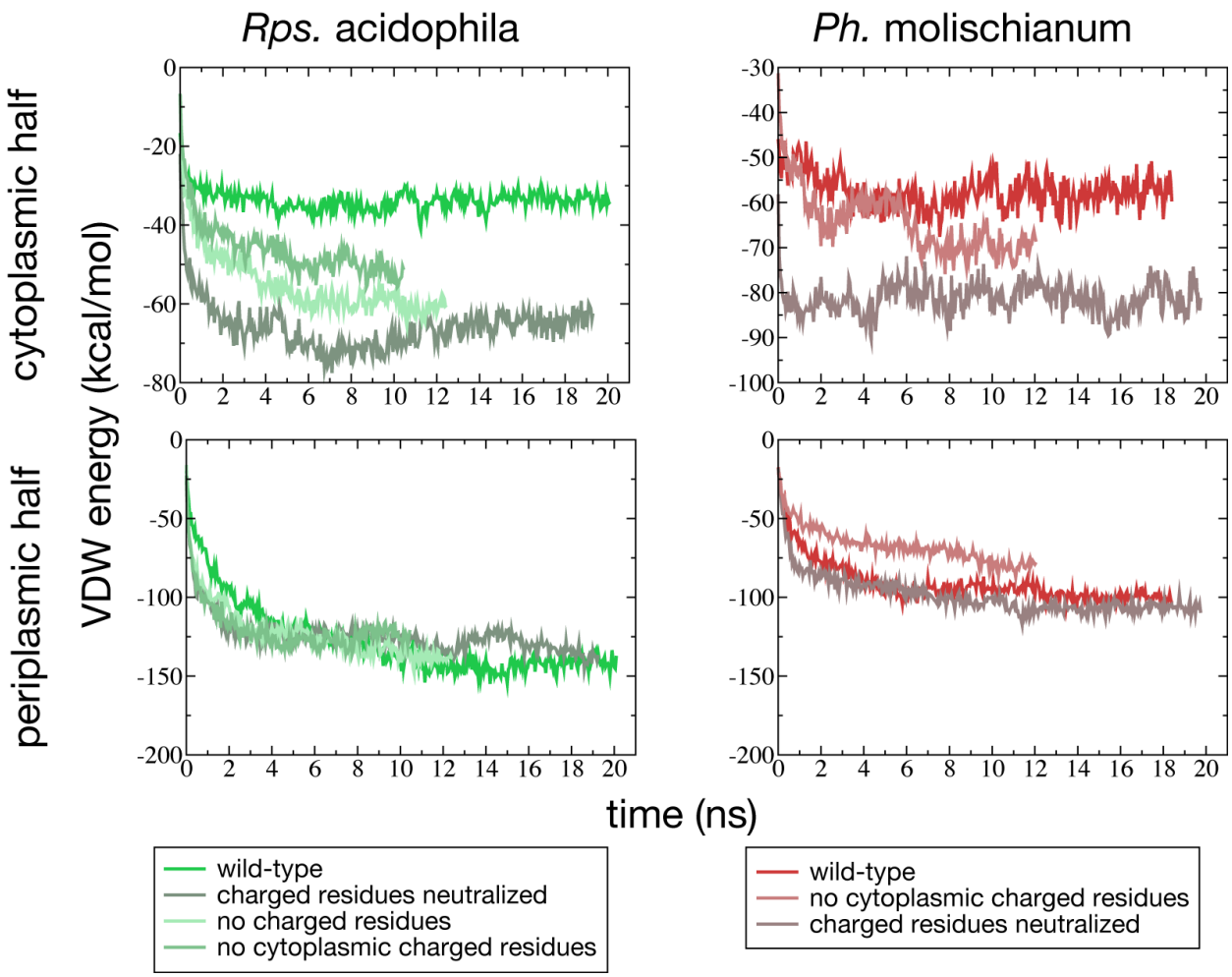

Figure S8: The van der Waals (VDW) energies for *Rps. acidophila* and *Ph. molischianum*. The top row shows the VDW energies for the cytoplasmic half of LH2; here the wild-type LH2s have higher VDW energies than their modified counterparts, indicating a less optimal packing on the top. The bottom row shows the VDW energies for the periplasmic half; here differences between wild-type and modified proteins are small.